

**A Numerical Approach of Slip Conditions Effect on Nanofluid Flow over a Stretching Sheet under Heating Joule Effect**

Hafiz Abdul Wahab<sup>1\*</sup>, Hussan Zeb<sup>1</sup>, Saira Bhatti<sup>2</sup> Muhammad Gulistan<sup>1</sup> and Sarfaraz Ahmad<sup>3</sup>

<sup>1</sup>Department of Mathematics & Statistics, Hazara University, Mansehra

<sup>2</sup>Department of Mathematics, COMSATS University Islamabad, Abbottabad Campus

<sup>3</sup>Department of Mathematics, AUST, Abbottabad

Email corresponding author: wahab@hu.edu.pk

Received: 03 September, 2018 / Accepted: 09 November, 2018 / Published online: 05 March, 2019

**Abstract.** In this analysis, we considered the effects of Joule heating and partial slip boundary conditions on time dependent mixed convective nanofluid flow over a stretching sheet along with heat source/sink. The governing model is transformed into the system of nonlinear ODE's by using the well known transformations. In order to calculate the physical quantities of the problem, we use the higher order convergence method, called shooting method followed by Runge-Kutta Fehlberg method. The importance of different physical parameters on velocity, temperature and concentration profiles are calculated numerically. The parameters of engineering interest i.e, skin fraction, Nusselt and Sherwood numbers are also calculated. Finally, we concluded that the velocity profiles decrease by increasing values of  $A$  and  $M$ . Moreover the variation of temperature, velocity and concentration profiles are analyzed for the different physical parameters.

**AMS (MOS) Subject Classification Codes:** 35S29; 40S70; 25U09

**Key Words:** Shooting method; MHD boundary layer flow; nanofluid flow; Joule heating; partial slip conditions.

## 1. INTRODUCTION

The investigation of the boundary layer pseudo plastic fluids has been of a great interest because it has many practical usage in industry such as emulsion coated sheets like photographic film, extrusion of polymer sheets, e tc. In order to examine the rheological assents of fluids, the Navier-Stokes equations are insufficient alone. Therefore, rheological models are implemented to reduced this problem. The description of non-Newtonian fluids

does not exist in single constitutive relationship between stress and strain. Due to their industrial and physiological applications, the non-Newtonian fluids have gained tremendous attraction. A plenty of applications in various built-up processing and biological fluids, an interest in boundary layer non-Newtonian fluid is increased significantly. A Few examples are drilling mud, plastic polymer, hot rolling, optical fibers, metal spinning, paper production and cooling of metallic plates. The investigation of the flow due to extending surface in a moving liquid is important in advanced industry. For example, the expulsion of metals and plastics, glass blowing, cooling or drying of papers, etc. The problems of linear stretching sheet for many events of fluid have also been investigated by many researchers. Sakiadis *et al.* [34] examined the boundary layer flow over a stretching surface. Various authors have discussed the different features of the flow over a movable plates. Vlegaar [36] studied the boundary layer on the stretching surface almost proportional to the distance from the orifice. Carn [14] studied Newtonian fluid flow layer over a stretching sheet on the uniform stress.

The magnetohydrodynamics of an electrically conducting fluid is an important phenomena used in metallurgical and modern metal-working. The electrical furnace metal can be fused by using the magnetic field and In a nuclear reactor containment boat, the wall of nuclear reactor is cooled down by applying magnetic field. MHD term was first proposed by Swedish electrical engineer, Alfve [5] in 1942. MHD equations are the combination of Maxwell's equations of electromagnetism, continuity equation and Navier-Stokes equations. If the electrically conducting liquid placed in a static magnetic field, the fluid movement pushes currents that create forces on the fluid. Equations that describe the MHD flow are a mixture of continuity equation, Navier Stokes equations and Maxwell's equations in fluid dynamics. Zeb *et al.* [39] we studied the effect of thermal radiation on time dependent fluid flow over a stretching sheet with variable thermal conductivity. Zeb *et al.* [40] studied the effect of thermal radiation and slip boundary condition on time dependent fluid flow over a stretching sheet along with variable thermal conductivity. Hussain *et al.* [20] investigated the impact of thermal radiation on bioconversions model for magnetohydrodynamics squeezing flow of nanofluid with heat and mass transfer between parallel surface. Time dependent MHD oscillating and rotating flow of Maxwell fluid in a cylinder subject to shear stress on the boundary was analyzed by Zafar *et al.* [38]. Mukhopadhyay *et al.* [25] investigated the effects of Joule heating on magnetohydrodynamics Newtonian fluid flow over a stretching sheet by placing between suction and junction. Raju *et al.* [30] analyzed the MHD free convective with porous medium by taking horizontal channel assuming insulated and incompressible bottom wall with the effect of heating joule and viscous dissipation. Ahmad *et al.* [4] examined quasi-linearization for unsteady MHD in heat and mass transfer flow of nanofluid over stretching sheet. Huichu [19] analyzed the unsteady MHD boundary layer flow over a stretching sheet along with frictional and Ohmic heating. Malik, *et al.* [23] investigated the magnetohydrodynamics stagnation point flow over a stretching sheet by assuming the convective boundary condition. MHD time dependent flow of a burger fluid past a circular cylinder along with porous medium was studied Safadar *et al.* [32]. the chemically reacting of incompressible fluid over an vertical plates was discussed by Awan *et al.* [9]. Sadiq *et al.* [33] discussed the exact solution of unsteady flow of Oldroyd-B fluid placed in a circular cylinder. Awan [8] analysed the exact solution for the time dependent flow of Maxwell fluid is placed in coaxial cylinder. Ali *et al.* [6]

investigated the influence of Magnetohydrodynamic electrically conducting oscillating and Rotating flows of Maxwell Fluids in a porous medium.

Another type of fluid is nanofluids which is measured by dispersing of small sized materials such as nanotubes, nanofibers, nanowires, droplets, nanosheet and nanorods. The nano-fluids are nanoscale colloidal suspensions containing condensed nanomaterials. The study of nanofluids has been a topic of intense research during the last one decade due to their interesting thermophysical properties and anticipated applications in heat transfer. The thermal conductivity of equal sample colloidal stable dispersed of nanofluids were obtained by using different experimental methods reported by the International Nanofluid Property Benchmark Exercise (INPBE). Nanotechnology has been commonly used in engineering since materials with size of nanometers possess unique chemical and physical properties. Tested nanofluids in the above study were based on aqueous and nonaqueous base-fluids and many others. In the above analysis, the data has been taken from most of the organization with in a relatively narrow based ( $\pm 10\%$  or below) about the sample mean with little outliers. It is found that the thermal conductivity of nano-fluids enlarges with increase in particle concentration and aspect ratio, as expected from classical theory, among various experimental approaches; small systematic differences in the absolute values of the nano-fluid thermal conductivity are obtained while such differences tend to disappear when the data are normalized to measure thermal conductivity of the base-fluids. Further explanation can be found in work by Jacopo *et al.* [11]. The evaluation of convective boundary conditions on MHD boundary layer nanofluid over a stretching sheet was found by Ishak *et al.* [10]. The steady flow of a third grade fluid in a porous half space was found by Karimi *et al.* [21] via rational Bernstein collocation method.

The phenomena of velocity slip has been discussed under different cases by using non-adherence of the fluid to solid boundary in [37]. Time dependent rotational flow of a second grad fluid with caputo time fractional derivative was examined by Raza *et al.* [31]. The viscous fluid is normally sticks to the boundary, for example, particulate fluid, rare field gas and many more which are discussed in [35]. The consequences of the slip condition plays a vital rule in the field of scientific, industrial and biological applications such as the internal cavities and artificial polishing of heart valves [24]. The most important study taken into the account is the slip boundary conditions over stretching sheets were carried out by Anderson [7]. Ibrahim *et al.* [17] analyzed magnetohydrodynamics boundary layer flow and heat transfer of nanofluid by assuming permeable stretching sheet taking the effect of slip boundary conditions. Poornima *et al.* [28] find out the effect of radiation on convection boundary layer flow due to a non linear stretching sheet. Rmaa Bhargava and Mania Goyal [12] simulate the consequences of velocity slip on MHD nanofluid with heat generation over a stretching sheet. The event of entropy generation on magnetohydrodynamics nanofluid flow over a stretching sheet under the considering velocity slip condition with heat generation was found out by Govindaraju *et al.* in [16]. Malik *et al.* [22] explained the magnetohydrodynamics and mixed convection flow of Eyring-Powell nanofluid by assuming the stretching sheet. Ndeem *et al.* [26] proposed a numerical studied viscoelastic nanofluid for two-dimensional stagnation point flow. They found influence of the embedded parameters. They used viscoelastic nanofluid for the controlling heat transfer from the sheet. Therefore, many ways were taken for improving the thermal conductivity of these fluids through suspension nano/micro or large-sized material particles in the fluid. Duwairi

[15] discussed the influence of Joule heating on the forced convection flow with thermal radiation. Partha *et al.* [27] reported that the events of the radiation on mixed convection heat transfer from an exponentially stretching surface under the consideration of viscous dissipation. Abro *et al.* [2] analyzed MHD generalized burger fluid over a permeable plates. Reddy [29] studied the viscous dissipation and thermal radiation on MHD flow due to a stretching sheet. MHD second grade unsteady flow of heat transfer with porous medium by using caputo-fabrizio fractional derivative was found by Abro *et al.* [1]. Abelman *et al.* [3]. analyzed the analytical solution of magnatohydrodynamics rotating and oscillating flow of a Maxwell fluid electrically conducting in a porous medium. Bhuiyan *et al.* [13] reported the Joule heating effects on MHD natural convection flows being with viscous dissipation from a horizontal circular cylinder. Ishaq *et al.* [18] examined time dependent MHD flow nanofluid film of an eyring Powell Fluid over a porous Stretching Sheet

From the above literature review, it is confirmed that no attempt has been made to the effect of heat source/sink on time dependent mixed convective nanofluid and heat transfer over a stretching sheet with Joule heating. We have successfully computed the solution of the coupled ordinary differential equations via numerical scheme through shooting method followed by Runge-Kutta Fehlberg method. The variation of different physical aspects are presented through graphs. Also, we obtained the numerical results for local skin fraction, heat transfer rate and Sherwood number by various different parameters (discussed in tables).

## 2. MATHEMATICAL MODEL

Let us consider an unsteady MHD incompressible mixed convective Nano-fluid flow over a stretching sheet along with partial slip condition. The flow is produced by a stretching sheet. The flow is in the region  $y > 0$  and subjected to a non-uniform magnetic field of strength  $B = B_0\sqrt{1 - \gamma_1\bar{t}}$  applied normally to the sheet,  $B_0$  is the initial strength of the magnetic field; see in the Fig 1. The fluid and heat flows are initiated at time zero. The sheet emerges out of a slit at origin  $x = 0, y = 0$  and moves with non-uniform velocity  $u_w(x, \bar{t}) = \frac{a_1x}{1-\gamma_1\bar{t}}$ , where  $a_1$  and  $\gamma_1$  are positive constants with dimensions of  $\bar{t}^{-1}$ , and  $a_1$  is the initial stretching rate.

$$\frac{\partial \bar{u}}{\partial x} + \frac{\partial \bar{v}}{\partial y} = 0, \quad (2.1)$$

$$\frac{\partial \bar{u}}{\partial \bar{t}} + \bar{u} \frac{\partial \bar{u}}{\partial x} + \bar{v} \frac{\partial \bar{v}}{\partial y} = \nu \frac{\partial^2 \bar{u}}{\partial y^2} - \frac{\sigma \beta^2 \bar{u}}{\rho} + [\beta_T(\bar{T} - \bar{T}_\infty) + \beta_C(C - C_\infty)]g, \quad (2.2)$$

$$\begin{aligned} \frac{\partial \bar{T}}{\partial \bar{t}} + \bar{u} \frac{\partial \bar{T}}{\partial x} + \bar{v} \frac{\partial \bar{T}}{\partial y} &= \frac{k}{\rho c_p} \frac{\partial^2 \bar{T}}{\partial y^2} + \sigma \frac{B_0^2}{\rho} \bar{u}^2 + \tau [D_B \left( \frac{\partial C}{\partial y} \frac{\partial C}{\partial y} \right) + \left( \frac{D_{\bar{T}}}{\bar{T}_\infty} \right) \left( \frac{\partial \bar{T}}{\partial y} \right)^2] \\ &+ \frac{Q}{\rho c_p} (T - T_\infty), \end{aligned} \quad (2.3)$$

$$\frac{\partial C}{\partial \bar{t}} + \bar{u} \frac{\partial C}{\partial x} + \frac{\partial \bar{T}}{\partial y} = D_B \left( \frac{\partial^2 C}{\partial y^2} \right) + \tau [D_B \left( \frac{D_{\bar{T}}}{\bar{T}_\infty} \right) \left( \frac{\partial^2 \bar{T}}{\partial y^2} \right)] \quad (2.4)$$

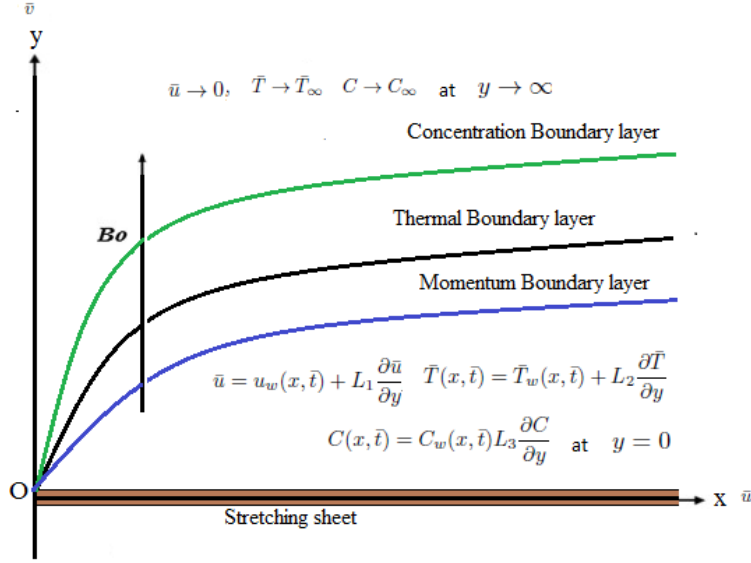


FIGURE 1. Geometry of the problem

subjected to the boundary conditions

$$\bar{u} = u_w(x, \bar{t}) + L_1 \frac{\partial \bar{u}}{\partial y}, v = 0, \bar{T}(x, \bar{t}) = \bar{T}_w(x, \bar{t}) + L_2 \frac{\partial \bar{T}}{\partial y}, C(x, \bar{t}) = C_w(x, \bar{t}) + L_3 \frac{\partial C}{\partial y}$$

as  $y = 0, \bar{u} \rightarrow 0, \bar{T} \rightarrow \bar{T}_\infty, C \rightarrow C_\infty$  at  $y \rightarrow \infty$ . (2.5)

Here,  $\bar{u}$  and  $\bar{v}$  the velocity components along the  $\bar{x}$  and  $\bar{y}$  - directions, respectively,  $\mu$  denotes viscosity,  $\rho$  represents the density,  $\beta_T$  - the coefficient of volumetric thermal expansion,  $\bar{T}$  denotes the temperature,  $C$  represents the concentration,  $\beta_C$  denotes coefficient of volumetric concentration expansion,  $\bar{T}_w$  and  $C_w$ - the temperature and concentration along the stretching sheet,  $\bar{T}_\infty$  and  $C_\infty$ - the ambient temperature and concentration,  $D_T$  - the thermophoresis coefficient,  $D_B$  - the Brownian diffusion coefficient,  $k$  - the thermal conductivity, and  $\tau$  represents the ratio of effective heat capacity and heat capacity of the fluid. Using the stream function  $\varphi(x, y)$  the continuity equation equation (2.1) is satisfied identically for the velocity component  $\bar{u}$  and  $\bar{v}$  specified as

$$\bar{u} = \frac{\partial \psi}{\partial y}, \bar{v} = -\frac{\partial \psi}{\partial x}. \quad (2.6)$$

The similarity variables are defined as follows:

$$\eta = \sqrt{\frac{a_1}{v(1 - \gamma_1 \bar{t})}} y, \quad (2.7)$$

$$\theta(\eta) = \frac{\bar{T} - \bar{T}_\infty}{\bar{T}_w - \bar{T}_\infty}, \quad (2.8)$$

$$\phi(\eta) = \frac{C - C_\infty}{C_w - C_\infty}, \quad (2.9)$$

$$= \sqrt{\frac{a_1 v}{(1 - \gamma_1 t)}} x h(\eta). \quad (2.10)$$

By substituting the above similarity transformation equations (2.1)–(2.4) are reduced at the form:

$$h''' + hh'' - h'^2 - Mh' - A(h' + \frac{1}{2}\eta h'') + \lambda_1 \theta + \lambda_2 \phi = 0, \quad (2.11)$$

$$\frac{1}{Pr} \theta'' + h' \theta - h \theta' - A(\theta + \frac{1}{2}\eta \theta') + \delta \theta + N_b \phi' \theta' + N_t (\theta')^2 + EcM^2 (h')^2 = 0, \quad (2.12)$$

$$\phi'' + Le h' \phi - Le h \phi' - ALe(\phi + \frac{1}{2}\eta \phi') + \frac{N_b}{N_t} (\theta'') = 0. \quad (2.13)$$

Subject to boundary conditions

$$h(0) = 0, \quad h'(0) = 1 + k_1 h''(0), \quad \theta(0) = 1 + k_2 \theta'(0), \quad \phi(0) = 1 + k_3 \phi'(0),$$

$$h'(\infty) = 0, \quad \theta(\infty) = 0, \quad \phi(\infty) = 0,$$

Where  $g'$  is the dimensionless velocity,  $\theta$  denotes the temperature,  $\phi$  represents the concentration  $\eta$  denotes the similarity variables where  $A = \frac{\gamma_1}{a}$  is the unsteady parameter,  $M = \frac{\sigma(B_0)^2}{\rho a}$  is magnetic parameter,  $Pr = \frac{\mu C_p}{k_\infty}$  is Prandtl number,  $Re_y = \frac{u_w \sqrt{y}}{\nu}$  Reynolds number,  $Le = \frac{\nu}{D_b}$  the Lewis number,  $K_r = \frac{k_0}{b}$  the reaction rate parameter,  $N_b = \frac{\tau D_B}{\nu} (C - C_\infty)$  the Brownian motion parameter,  $\lambda_1 = \frac{Gr}{Re^3/2_x}$ , the local thermal Grashof number  $\lambda_2 = \frac{Gm}{Re^3/2_x}$ , -the local concentration Grashof number,  $\bar{Re}_x = \frac{\bar{u}_w \bar{x}}{\nu}$  is the local Reynolds number,  $k_1 = L_1 \sqrt{\frac{a_1}{1 - \gamma_1 t}}$  represents the velocity slip factor,  $L_1$  represents the initial value of velocity slip factor,  $k_2 = L_2 \sqrt{\frac{a_1}{1 - \gamma_1 t}}$  denotes the thermal slip factor,  $L_2$  is the initial value of thermal slip factor,  $k_3 = L_3 \sqrt{\frac{a_1}{1 - \gamma_1 t}}$  represents the mass slip factor,  $L_3$  is the initial value of mass slip factor, if  $Q$  is negative it will be a heat sink if  $Q$  is positive then it will be heat source. The condition of the no-slip case is attained when  $k_1 = k_2 = k_3 = 0$ . The quantities  $C_f$ ,  $Nu_{\bar{x}}$  and  $Sh_{\bar{x}}$  are define by

$$C_f = \frac{\tau_w}{\rho u_w^2} \quad (2.14)$$

$$Nu_x = \frac{x q_w}{k(\bar{T}_w - \bar{T}_\infty)}, \quad (2.15)$$

$$Sh_x = \frac{x j_m}{D_B(C_w - C_\infty)}, \quad (2.16)$$

where  $\tau_w$  is the skin friction or shear stress along the stretching surface,  $q_w$  the heat flux and  $j_m$  the concentration flux from the surface and are given by

$$\tau_x = \mu \frac{d\bar{u}}{dy} \Big|_{y=0} \quad q_w = [-k \frac{d\bar{T}}{dy}]_{y=0} \quad j_m = [-D_B \frac{dC}{dy}]_{y=0}. \quad (2.17)$$

where  $u_w$ ,  $q_m$  and  $q_w$ , are the wall shear stress, mass fluxes and heat transfer respectively. In dimensionless form, In dimensionless form, the reduced local Nusselt and Sherwood numbers can be written as

$$C_f \sqrt{Re_x} = h''(0), \quad \frac{Nu_x}{\sqrt{Re_x}} = -\theta'(0), \quad \frac{Sh_x}{\sqrt{Re_x}} = -\phi'(0). \quad (2. 18)$$

### 3. SHOOTING METHOD FOR THE PROPOSED MODEL

Eqs ( 2. 11 ) – ( 2. 13 ) are the system of nonlinear, 3rd order in  $h$ , 2nd order in  $\theta$  and 2nd order in  $\phi$  respectively. First of all these non-linear ODE's are reduce into a system of first order ODE's and then solved by using shooting method. The equations ( 2. 11 ) – ( 2. 13 ) can be written as:

$$h''' = -hh'' + Mh' + h'^2 + A(h' + \frac{1}{2}\eta h'') - \lambda_1\theta - \lambda_2\phi, \quad (3. 19)$$

$$\theta'' = Pr[-h'\theta + h\theta' + A(\theta + \frac{1}{2}\eta\theta') - \delta\theta - N_b\phi'\theta' - N_t(\theta')^2 - EcM^2(h')^2], \quad (3. 20)$$

$$\phi'' = Le(-h'\phi + h\phi' + A(\phi + \frac{1}{2}\eta\phi')) - \frac{N_b}{N_t}\theta''. \quad (3. 21)$$

To convert these higher order nonlinear ODE's into system of first order ODE's, let

$$h = u_1, \quad h' = u_2, \quad h'' = u_3, \quad h''' = u_3 \text{ and } h''' = u_3', \quad (3. 22)$$

$$\theta = u_4, \quad \theta' = u_5 \text{ and } \theta'' = u_5' \quad (3. 23)$$

$$\phi = u_6, \quad \phi' = u_7 \text{ and } \phi'' = u_7' \quad (3. 24)$$

The nonlinear coupled ODE's are converted into a system o first order simultaneous algebraic form, which can be defined as form a

$$u_1' = u_2, \quad (3. 25)$$

$$u_2' = u_3, \quad (3. 26)$$

$$u_3' = -u_1u_3 + u_2^2 + Mu_2 + A(u_2 + \frac{1}{2}\eta u_3) - \lambda_1u_4 - \lambda_2u_6, \quad (3. 27)$$

$$u_4' = u_5, \quad (3. 28)$$

$$u_5' = -u_2u_4 + u_1u_5 + A(u_4 + \frac{1}{2}\eta u_5) - \delta u_4 - N_b u_7 u_5 - N_t u_5^2 - EcMu_2^2 \quad (3. 29)$$

$$u_6' = u_7, \quad (3. 30)$$

$$u_7' = -Leu_2u_6 + Leu_1u_7 + ALe(u_6 + \frac{1}{2}\eta u_7) - \frac{N_b}{N_t}[u_5']. \quad (3. 31)$$

In the above equations, the prime denotes the derivative with respect to  $\eta$ . The boundary conditions are

$$\begin{aligned} u_1(0) = 0, \quad u_2(0) = 1 + k_1u_3(0), \quad u_4(0) = 1 + k_2u_5(0), \quad u_6(0) = 1 + k_3u_7(0) \\ u_2(\infty) = 0, \quad u_4(\infty) = 0, \quad u_6(\infty) = 0 \end{aligned} \quad (3. 32)$$

To determine the solution of system of seven ODE's ( 3. 25 ) – ( 3. 31 ) by using shooting method, seven initial assumptions are required, but in system ( 3. 32 ), two initial guesses are given in  $h$ , one in  $\theta$  and one in  $\phi$  and the other three conditions are defined as  $\eta \rightarrow \infty$ .

These three conditions generate result in three unknowns. The subsequent and foremost step of this method is choosing the estimated values of  $\eta$  at  $\infty$ . The solution process is initiated with certain initial guesses and finding out the solution of (BVP) including governing model. The method of solution with a new values of  $\eta$  at  $\eta \rightarrow \infty$  and the method is repeated until two consecutive values of  $g''(0)$ ,  $\theta'(0)$  and  $\phi'(0)$  are different only after the significant digits. Thus final values of  $\eta$  are considered as  $\eta \rightarrow \infty$ .

#### 4. RESULTS AND DISCUSSION

The variation of different physical aspects are presented through graphs (as shown in Figs 2–19). The influence of unsteady parameter is shown in Fig: 2 on the velocity and temperature profiles. Fig 3 is for the variation of velocity and temperature profiles for values of  $M$ . A decrease in variation of velocity and temperature profiles increases by enlarge values of  $M$ . Fig: 4 plotted for the distribution of concentration profile for the distinct values of  $M$  and  $A$  respectively. The decreases the concentration profile by increasing values of  $M$  and  $A$ . Figure 5 plotted for the distribution of concentration and temperature profiles for the distinct values of  $Pr$ . The temperature profile decreases and concentration profile increases by increasing values of  $Pr$ . Figure 6 designated for the velocity and temperature profiles for the different values of  $\lambda_1$ . The increase in the velocity profile and decrease in temperature profile by increasing the values of  $\lambda_1$ . Figure 7 indicates the variation of velocity and temperature profiles for the various values of  $\lambda_2$ . The result has shown the step down the velocity and temperature profiles by the step up values of  $\lambda_2$ . Figure 8 shows the distribution of the temperature profile for the various values of the  $N_t$  and  $N_b$ . The result has show that the temperature profile decreases by increasing values of thermophoresis  $N_t$  and Brownian motion parameters  $N_b$ . The Figure 9 shows that the influence of Ecklet number  $E_c$  on temperature and concentration profiles. The result shows that the temperature profile increases and reduced the concentration profile by the step up values of  $E_c$ . Figure 10 designated for the distribution of the concentration profile for values of  $L_e$  on the concentration profile. The result shows that a decrease in concentration profile as the  $L_e$  increases. This is due to the fact that there is a decrease in the nanoparticle volume fraction boundary layer thickness with the increase in the Lewis number. Figure 11 shows the variation of the concentration profile for the distinct values of  $N_b$ . It is noticed that the concentration profile is reduced by incrementing value in Brownian motion  $N_b$ . The effect of the thermophoresis parameter  $N_t$  on the concentration of the flow field is show in Figure 12. We observe that the behavior of  $N_t$  indicates a cold surface while negative to a hot surface. It is seen that the concentration decreases, as the thermophoresis parameter increases. The variation of velocity slip parameter  $k_1$  on the velocity profile is shown in Figure 13. The result shows that the velocity graph is reduced with the step up values of velocity slip parameter  $k_1$ . Figure 14 is plotted for the distinction of the temperature profile for the different values thermal slip parameter  $k_2$ . On observing this figure, the temperature graph is reduced as the value of temperature slip parameter  $k_2$  increase. Figure 15 is plotted for the influence of the solutal slip parameter  $k_3$  on the concentration profile. The result has shown that the concentration profile is reduced by the step up value of solutal slip parameter  $k_3$ . Figure 16 represents the temperature profile with using different value for the heat source parameter. If we increase the value of the heat source, then the temperature profile increases. Heat source provides extra heat to the sheet which increases its temperature.

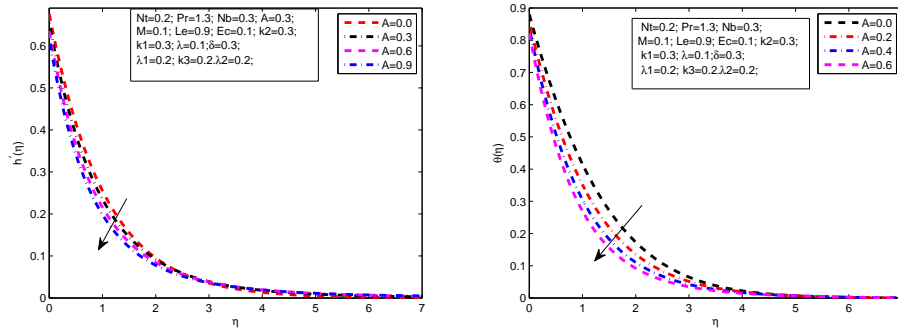


FIGURE 2. The variation of  $h'$  and  $\theta$  for distinct values of  $A$ .

This increment is responsible for the increment of the thickness of the thermal boundary layer. Figure 17 is plotted for the temperature profile with the use of different values for the heat sink parameter. If we increase the values of the heat sink, then the temperature profile decreases. This implies that it removes heat from the sheet which decreases thickness of the boundary layer. Figure 18 represents the concentration profile by using different values for the heat source parameter. If we step up the value of the heat source, then the concentration profile decreases. Figure 19 is plotted for the concentration profile with the use of different values for the heat sink parameter. If we increase the value of the heat sink then concentration profile increases. Table 1–2 is prepared for the influence of various parameters on skin friction  $C_f$ , Nusselt number  $Nu_x$  and Sherwood numbers  $Sh$ . Table 1 shows that heat skin friction increases with an increase in  $M$ ,  $A$ ,  $Pr$ ,  $\delta$ ,  $L_e$  and  $\lambda_1$ . The skin friction steps up by the incrementing values of  $N_b$ .  $Nu_x$  increases with an increase in  $M$ ,  $\delta$ , and  $L_e$ .  $Nu_x$  steps down by increasing values of  $Pr$ ,  $A$ ,  $L_e$  and  $\lambda_1$ . Sherwood number  $Sh_x$  increases by the incrementing values of  $A$ ,  $Pr$ ,  $N_b$ , and  $\lambda_1$ . Sherwood number  $Sh_x$  is reduced by increasing values of  $M$ ,  $\delta$  and  $L_e$ . The Table 2 shows that the skin friction steps up by incrementing the values of  $\lambda_2$ ,  $N_t$ ,  $k_1$  and  $k_3$ . Skin friction increments by the incrementing the values of  $k_2$ .  $Nu_x$  increases with an increase in  $\lambda_2$ ,  $N_t$   $k_2$  and  $Ec$ .  $Nu_x$  reduces by increasing values of  $k_1$  and  $k_3$ . Sherwood number  $Sh_x$  steps up with an increment in  $k_1$  and  $k_3$ . Sherwood number  $Sh_x$  decreases by increasing values of  $\lambda_2$ ,  $N_t$ ,  $k_2$  and  $Ec$ .

## 5. CONCLUSIONS AND FUTURE WORK

The present work is the analysis of an unsteady incompressible magnetohydrodynamics boundary layer flow heat transfer and a nanofluid over a stretching sheet under the effect of slip boundary conditions and heating joule in the existence of heat source or sink has been considered. We use similarity transformation for transforming the nonlinear coupled ordinary differential equations. We successfully computed the solution of coupled ordinary differential equations via numerical scheme through shooting method followed by Runge-Kutta Fehlberg method. The behaviour of various parameters on velocity, temperature and

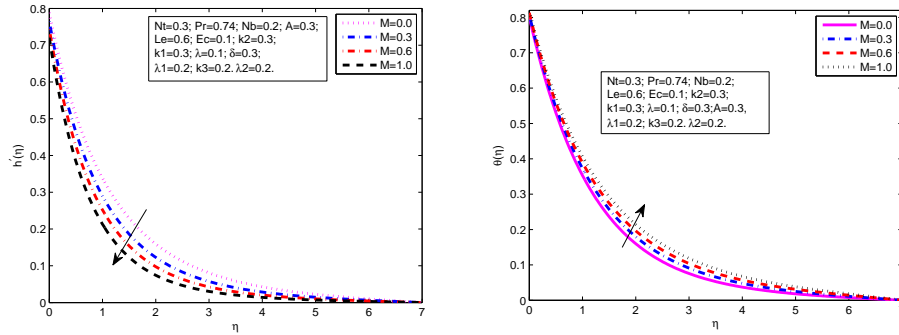


FIGURE 3. The variation of  $h'$  and  $\theta$  for distinct values of  $M$ .

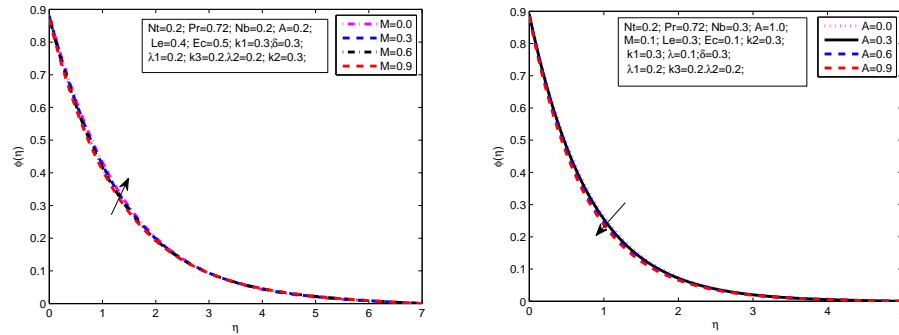


FIGURE 4. The variation of  $\phi$  for distinct values of  $M$  and  $A$ .

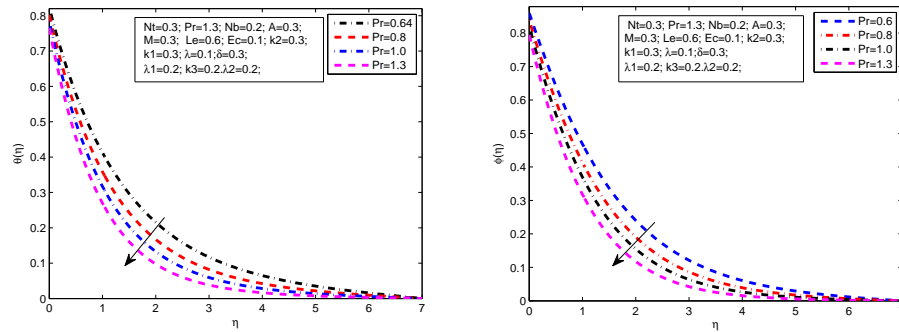


FIGURE 5. The variation of  $\theta$  and  $\phi$  for distinct values of  $Pr$ .

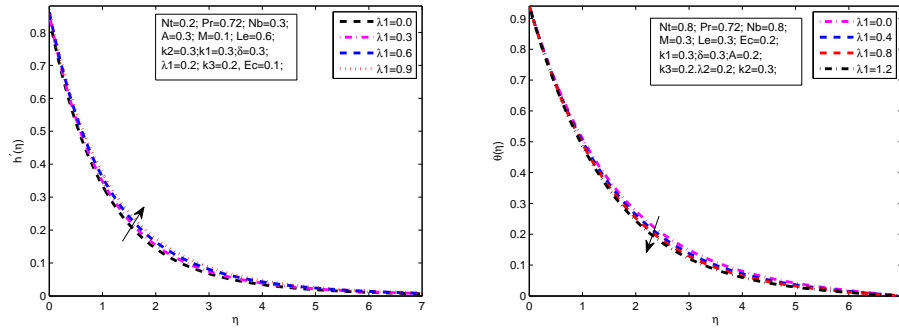


FIGURE 6. The variation of  $h'$  and  $\theta$  for distinct values of  $\lambda_1$ .

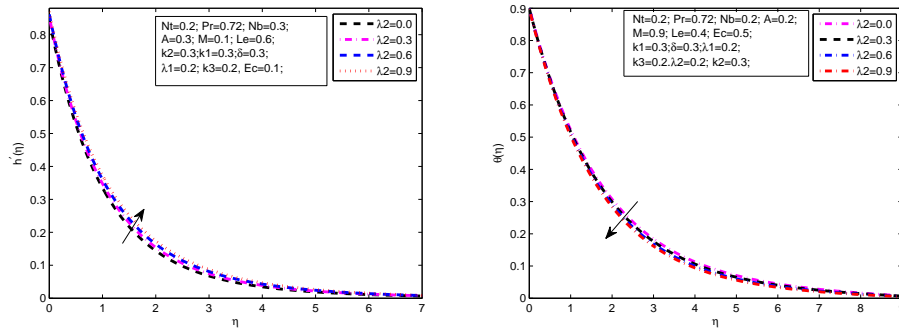


FIGURE 7. The variation of  $h'$  and  $\theta$  for distinct values of  $\lambda_2$

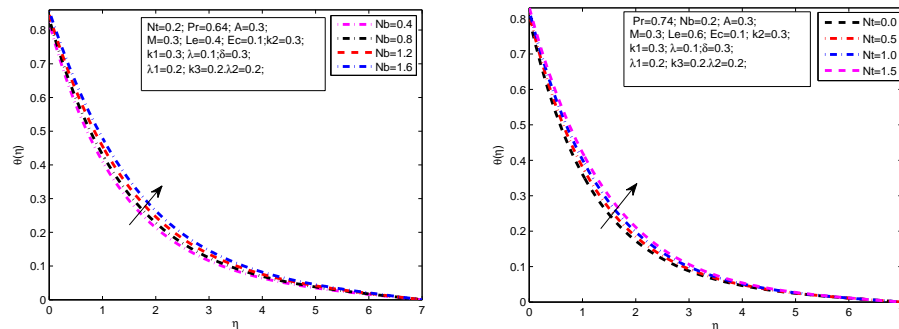


FIGURE 8. The variation of  $\theta$  for distinct values of  $N_b$  and  $N_t$  on  $\theta$ .

concentration profiles are shown graphically. The behaviour of the local skin friction coefficient, local Nusselt number and local Sherwood number are shown numerically through table. The major conclusions are listed below;

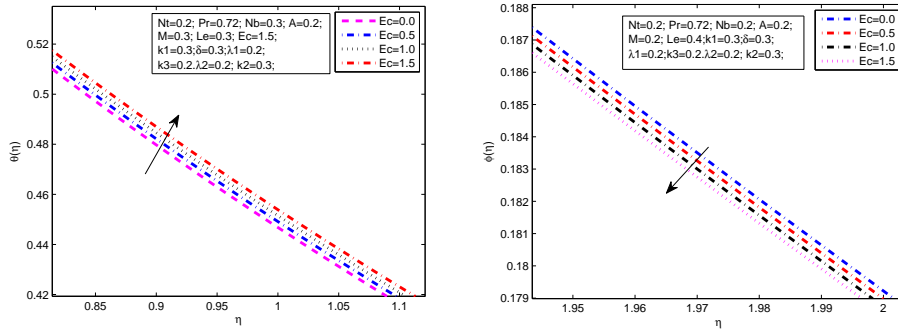


FIGURE 9. The variation  $\theta$  and  $\phi$  for distinct values of  $Ec$ .

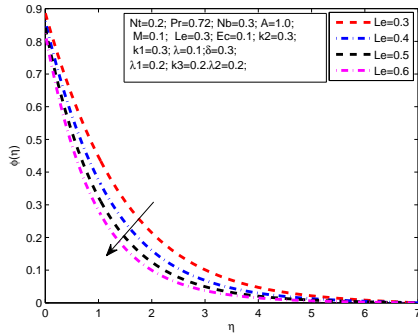


FIGURE 10. The variation of  $\phi$  for distinct values of  $Le$ .

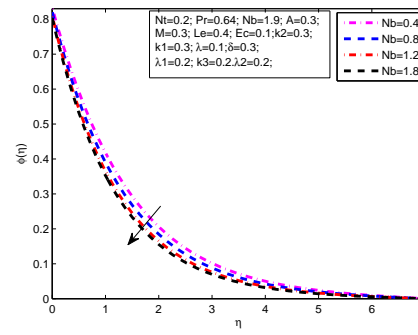


FIGURE 11. The variation of  $\phi$  for distinct values of  $N_b$ .

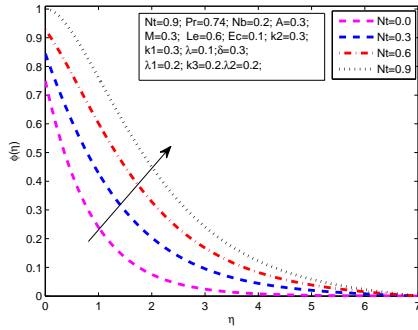


FIGURE 12. The variation of  $\phi$  for distinct values of  $N_t$ .

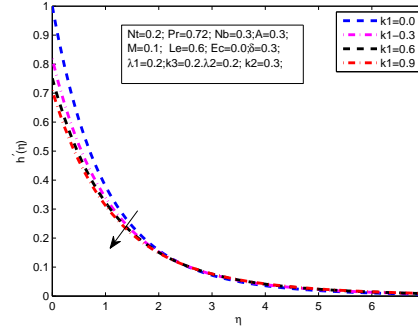


FIGURE 13. The variation of  $h'$  for distinct values of  $k_1$ .

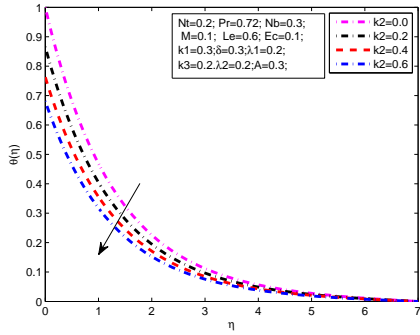


FIGURE 14. Influence of  $k_2$  on  $\theta$ .

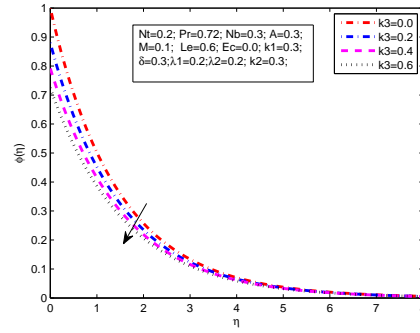


FIGURE 15. The variation of  $\phi$  for distinct values of  $k_3$ .

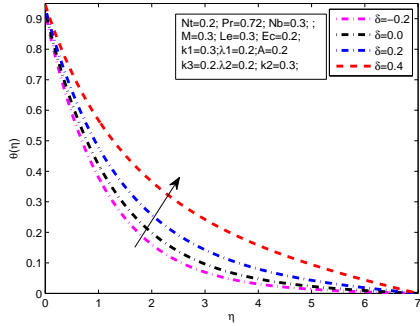


FIGURE 16. The variation of  $\theta$  for distinct values of  $\delta$ .

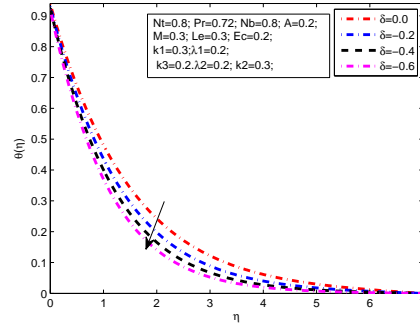


FIGURE 17. The variation of  $\theta$  for distinct values of  $\delta$ .

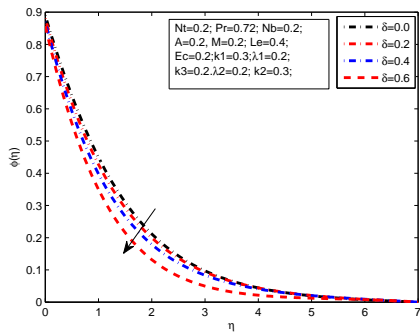


FIGURE 18. The behaviour of  $\delta$  on  $\phi$ .

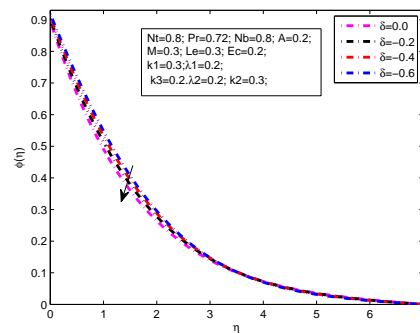


FIGURE 19. The behaviour of  $\delta$  on  $\phi$ .

$A$	$M$	$Pr$	$\delta$	$Le$	$N_b$	$\lambda_1$	$-h''(0)$	$-\theta'(0)$	$-\phi'(0)$
0.8	1.0	0.72	0.5	0.5	0.5	0.5	0.12222	0.57535	0.1318
							0.11130	0.48859	0.1543
							0.11417	0.51136	0.1480
							0.11695	0.53340	0.1422
							0.10736	0.58869	0.1285
							0.11053	0.58578	0.1292
							0.11359	0.58300	0.1299
							0.12099	0.53798	0.1417
							0.11989	0.50762	0.1495
							0.11900	0.48595	0.1548
							0.12480	0.68052	0.1023
							0.12427	0.65881	0.1084
							0.12372	0.63620	0.1148
							0.12314	0.61264	0.1214
							0.12247	0.57527	0.1269
							0.12232	0.57531	0.1299
							0.12217	0.57537	0.1328
							0.12000	0.61117	0.1638
							0.12189	0.68796	0.1373
							0.12241	0.66397	0.1282
							0.0	0.57135	0.1327
							0.2	0.57297	0.1324
							0.4	0.57456	0.1320

TABLE 1. Effect of  $A$ ,  $M$ ,  $Pr$ ,  $\delta$ ,  $Le$ ,  $N_b$  and  $\lambda_1$  on  $-h''(0)$ ,  $-\theta'(0)$  and  $-\phi'(0)$ 

- There is a decrease in velocity profile  $h'(0)$  with increasing values of  $A$ ,  $\lambda_2$  and  $k_1$
- The velocity  $h'(0)$  profile increases by increasing values of the  $\lambda_1$ .
- There is an increase in temperature profile  $\theta(\eta)$  with the increasing value of  $M$ ,  $\lambda_2$ ,  $N_b$ ,  $N_t$ .
- There is a decrease in temperature  $\theta(\eta)$  profile with the increasing value of  $Pr$ ,  $\lambda_1$ ,  $Le$  and  $k_2$ .
- By increasing heat sink  $\delta$  temperature profile  $\theta(\eta)$  decreases and alternatively concentration  $\phi(\eta)$  profiles increase.
- The gradient of the temperature increases with the increase in heat source parameter  $\delta$  and alternatively concentration  $\phi(\eta)$  profiles decrease.
- The concentration profile  $\phi(\eta)$  increases with the incrementing values in magnetic parameter  $M$ ,  $k_1$ ,  $N_t$ ,  $Ec$ ,  $\lambda_1$  and  $Pr$ .
- The concentration profile  $\phi(\eta)$  is reduced with the step up values of  $N_b$ ,  $Le$ ,  $A$ ,  $k_3$  and  $\lambda_2$ .
- In future we will try to implement other numerical method for comparison of our analysis.

$\lambda_2$	$N_t$	$k_1$	$k_2$	$k_3$	$Ec$	$-h''(0)$	$-\theta'(0)$	$-\phi'(0)$
0.8	1.0	0.72	0.5	0.5	0.5	0.12222	0.57535	0.1318
	0.0					0.11801	0.57698	0.1315
	0.2					0.12054	0.57600	0.1317
	0.4					0.12306	0.57502	0.1319
		0.0				0.11576	0.51269	0.7546
		0.4				0.11650	0.48669	0.6464
		0.8				0.11697	0.46321	0.5599
			0.0			0.12235	0.58113	0.1302
			0.1			0.12222	0.57535	0.1318
			0.2			0.12209	0.59936	0.1335
				0.0		0.17092	0.59901	0.1268
				0.2		0.12222	0.57535	0.1318
				0.3		0.10736	0.56731	0.1336
					0.0	0.10336	0.57051	0.1578
					0.2	0.10558	0.51713	0.1441
					0.4	0.10736	0.56731	0.1336
					0.0	0.10874	0.57244	0.2149
					0.2	0.10637	0.60568	0.1620
					0.4	0.10494	0.62642	0.1298

TABLE 2. Effect of  $\lambda_2$ ,  $N_t$ ,  $k_1$ ,  $k_2$ ,  $k_3$ , and  $Ec$  on  $-h''(0)$ ,  $-\theta'(0)$  and  $-\phi'(0)$

## REFERENCES

- [1] K. A. Abro and M. A. Solangi, *Heat Transfer in Magnetohydrodynamic Second Grade Fluid with Porous Impacts using Caputo-Fabrizio Fractional Derivatives*, Punjab Univ. j. math. **49**, No. 2 (2017) 113–125.
- [2] K. A. Abro, M. Hussain and M. M. Baig, *A Mathematical Analysis of Magnetohydrodynamic Generalized Burger Fluid for Permeable Oscillating Plate*, Punjab Univ. J. Math. Vol. 50, No. 2 (2018) 97–111.
- [3] S. Abelman, E. Momoniat and T. Hayat, *Magnetohydrodynamic Oscillating and Rotating Flows of Maxwell Electrically Conducting Fluids in a Porous Plane*, Punjab Univ. j. math. **50**, No. 3 (2018) 61–71.
- [4] R. Ahmad and Waqar A. Khan, *Unsteady heat and mass transfer magnetohydrodynamic (MH) nanofluid flow over a stretching sheet with heat source/sink using quasi-linearization technique*, Canadian J. of Phy. **93**, No. 12 (2015) 1477–1485.
- [5] H. Alfve, *Existence of electromagnetic hydrodynamic waves*, J. Appl. Math. Phys. **150**, No. 3805 (1942) 405–506.
- [6] A. Ali, M. Tahir, R. Safdar, A. U. Awan, M. Imran and M. Javaid, *Magnetohydrodynamic Oscillating and Rotating Flows of Maxwell Electrically Conducting Fluids in a Porous Plane*, Punjab Univ. J. Math. Vol. 50, No. 4 (2018) 61–71.
- [7] H. I. Andersson, *Slip flow past a stretching surface*, Acta Mechanica **158**, No. 1–2 (2002) 121–125.
- [8] A. U. Awan, M. Imran, M. Athar and M. Kamran, *Exact analytical solutions for a longitudinal flow of a fractional Maxwell fluid between two coaxial cylinders*, Punjab Univ. j. math. **45**, (2013) 9–23.
- [9] A. U. Awan, R. Safdar, M. Imran and A. Shoukat, *Effects of Chemical Reaction on the Unsteady Flow of an Incompressible Fluid over a Vertical Oscillating Plate*, Punjab Univ. j. math. **48**, No. 2 (2016) 167–182.
- [10] N. Bachok, A. Ishak and I. Pop, *Boundary-layer flow of nano fluids over a moving surface in moving fluid*, Int. J. Ther. Sci. **48**, No. 9 (2010) 1663–1668.
- [11] Jacopo Buongiorno, and David C. Venerus, *A benchmark study on the thermal conductivity of nano fluids*, Journal of Applied Physics, **106**, No. 617 (2009) 094312–0943126.
- [12] R. Bhargava and M. Goyal, *Mhd non-newtonian nano fluid flow over a permeable stretching sheet with heat generation and velocity slip*, Int. Scholarly and Scientific Research and Innovation **8**, No. 6 (2008) 909–916.
- [13] A. S. Bhuiyan, N. H. M. A. Azim and M. K. Chowdhury, *Joule heating effects on MHD natural convection flows in presence of pressure stress work and viscous dissipation from a horizontal circular cylinder*, J. Appl. Fluid Mech. **7**, No. 1 (2014) 7–13.
- [14] J. L. Crane, *Flow past a Stretching Plate*, ZAMP. **21**, No. 4 (1970) 645–647.
- [15] H. M. Duwairi, *Fin placement for optimal forced convection heat transfer from a cylinder in cross flow*, Int. J. Numerical Methods for Heat and Fluid Flow **15**, No. 3 (2005) 277 – 295.
- [16] M. Govindaraju and N. V. Ganesh, *Entropy generation analysis of magneto hydrodynamic flow of a nano fluid over a stretching sheet*, J. Egyptian Math. Soc. **23**, No. 2 (2015) 429–434.
- [17] W. Ibrahim and B. Shankar, *MHD boundary layer flow and heat transfer of a nano fluid past a permeable stretching sheet with velocity thermal and solutal slip boundary conditions*, Computers and Fluids **75**, (2013) 1–10.
- [18] M. Ishaq, G. Ali, S. I. A. Shah, Z. Shah, S. Muhammad and S. A. Hussain, *Nanofluid Film Flow of Eyring Powell Fluid with Magneto Hydrodynamic Effect on Unsteady Porous Stretching Sheet*, Punjab Univ. J. Math. Vol. 51, No. 3 (2019) 147–169.
- [19] H. Hua and X. Su, *Unsteady mhd boundary layer flow and heat transfer over the stretching sheets submerged in a moving fluid with ohmic heating and frictional heating*, Open Phy. **13**, No. 1 (2015) 210–217.
- [20] S. A. Hussain, G. Ali, S. I. A. Shah, S. Muhammad and M. Ishaq, *Bioconvection Model for Magneto Hydrodynamics Squeezing Nanofluid Flow with Heat and Mass Transfer Between Two Parallel Plates Containing Gyrotactic Microorganisms Under the Influence of Thermal Radiations*, Punjab Univ. J. Math. Vol. 51, No. 4 (2019) 13–36.
- [21] K. Karimi and A. Bahadorimrhr, *Rational Bernstein Collocation Method for Solving the Steady Flow of a Third Grade Fluid in a Porous Half Space*, Punjab Univ. j. math. **49**, No. 1 (2017) 63–73.
- [22] M. Y. Malik, I. Khan, A. Hussain and T. Salahuddin, *Mixed convection flow of MHD Eyring powell nano fluid over a stretching sheet a numerical study*, AIP Advance **5**, No. 11 (2015), 117118–117121.
- [23] M. Y. Malik and T. Salahuddin, *Numerical solution of MHD stagnation point flow of williamson fluid model over a stretching cylinder*, Int. J. Nonlinear Sci. **16**, No. 3 (2015) 161–164.

- [24] S. Mansur and A. Ishak, *The magnetohydrodynamic boundary layer flow of a nano-fluid past a stretching/shrinking sheet with slip boundary conditions*, J. Appl. Math. (2014) 181–188.
- [25] S. Mukhopadhyay, *MHD boundary layer flow and heat transfer over an exponentially stretching sheet embedded in a thermally stratified medium*, Alex. Eng. J. **52**, No. 3 (2013) 259–265.
- [26] S. Nadeem, R. Mehmood and N. S. Akbar, *Non-orthogonal stagnation point flow of a nano nonNewtonian fluid towards a stretching surface with heat transfer*, Int. J. Heat and Mass Transfer **57**, No. 2 (2013) 679–689.
- [27] M. K. Partha, P. V. S. N. Murthy and G. P. Rajasekhar, *Effect of viscous dissipation on the mixed convection heat transfer from an exponentially stretching surface*, Heat Mass Transfer **41**, No. 4 (2005) 360–366.
- [28] T. Poornima and N. Bhaskar, *Radiation effects on MHD free convective boundary layer flow of nano fluids over a nonlinear stretching sheet*. *advances in applied science research*, Adv. Appl. Sci. Res. **4**, No. 2 (2013) 190–202.
- [29] M. G. Reddy, *Thermal radiation and chemical reaction effects on steady convective slip flow with uniform heat and mass flux in the presence of ohmic heating and a heat source*, J. Appl. Fluid Mech. **10**, No. 4 (2014) 417–442.
- [30] K. V. S. Raju, T. Sudhakar Reddy, M. C. Raju, P. V. Satya Narayana and S. Venkataramana, *MHD convective flow through porous medium in a horizontal channel with insulated and impermeable bottom wall in the presence of viscous dissipation and joule heating*, Ain. Shams Eng. J. **5**, No. 2 (2013) 543–551.
- [31] N. Raza, *Unsteady Rotational Flow of a Second Grade Fluid with Non-Integer Caputo Time Fractional Derivative*, Punjab Univ. J. Math. Vol. 49, No. 3 (2017) 15-25.
- [32] R. Safdar, M. Imran, M. Tahir, N. Sadiq and M. A. Imran, *MHD Flow of Burgers Fluid under the Effect of Pressure Gradient Through a Porous Material Pipe*, Punjab Univ. j. math. **50**, No. 4 (2018) 73-90.
- [33] N. Sadiq, M. Imran, R. Safdar, M. Tahir and M. Javai, *Exact Solution for Some Rotational Motions of Fractional Oldroyd-B Fluids Between Circular Cylinders*, Punjab Univ. J. Math. **50**, No. 4 (2018) 39-59.
- [34] B. C. Sakiadis, *Boundary layer behaviour on continuous solid surface, ii. the boundary layer on a continuous at surface*, J. Am. Inst. Chem. Eng. **7**, No. 2 (1969) 221–225.
- [35] V. P. Shidlovskiy, *Introduction to the dynamics of rarefied gases*, American Elsevier Publishing (1967).
- [36] J. Vleggaar, *Laminar boundary layer behaviour on continuous accelerating surface*, Chem. Eng. Sci., **32**, No. 12 (1977) 1517–1525.
- [37] Yoshimura and R. K. Prud, *Wall slip corrections for couette and parallel disk viscometry*, J. Rheo. **32**, No. 53 (1988) 53–67.
- [38] A. A. Zafar, M. B. Riaz and M. A. Imran, *Unsteady Rotational Flow of Fractional Maxwell Fluid in a Cylinder Subject to Shear Stress on the Boundary*, Punjab Univ. J. Math. Vol. 50, No. 2 (2018). 21-32.
- [39] H. Zeb, H. A. Wahab, M. Shahzad, S. Bhatti and M. Gulistan, *Thermal effects on MHD unsteady Newtonian fluid flow over a stretching sheet*, J. of Nano fluids. **7**, No. 5 (2018) 704–710.
- [40] H. Zeb, H. A. Wahab, M. Shahzad, S. Bhatti and M. Gulistan, *A numerical approach for the thermal radiation on MHD unsteady Newtonian fluid flow over a stretching sheet with variable thermal conductivity and partial slip conditions*, J. of Nano fluids. **7**, No. 5 (2018) 870–878.